QUANTUM OPTICS

Metalens-array–based high-dimensional and multiphoton quantum source

Lin Li[1,2,3,4]*, Zexuan Liu[1,5,6]*, Xifeng Ren[7,8]*, Shuming Wang[1,5,6]*†, Vin-Cent Su[9], Mu-Ku Chen[2,3,10], Cheng Hung Chu[3,10], Hsin Yu Kuo[3,10], Biheng Liu[7,8], Wenbo Zang[1,6], Guangcan Guo[7,8], Lijian Zhang[1,5,6]†, Zhenlin Wang[1,6]†, Shining Zhu[1,5,6]†, Din Ping Tsai[2,3,10]†

The development of two-dimensional metasurfaces has shown great potential in quantum-optical technologies because of the excellent flexibility in light-field manipulation. By integrating a metalens array with a nonlinear crystal, we demonstrate a 100-path spontaneous parametric down-conversion photon-pair source in a 10 × 10 array, which shows promise for high-dimensional entanglement and multiphoton-state generation. We demonstrate two-, three- and four-dimensional two-photon path entanglement with different phases encoded by metalenses with fidelities of 98.4, 96.6, and 95.0%, respectively. Furthermore, four-photon and six-photon generation is observed with high indistinguishability of photons generated from different metalenses. Our metalens-array–based quantum photon source is compact, stable, and controllable, indicating a new platform for integrated quantum devices.

Quantum optical systems, benefiting from the fast speed, long coherence time, versatile controllability, and large information capacity of photons, is one of the most attractive physical systems for the investigation of quantum information processing. They are widely used in quantum communication (*1*–*4*), quantum computation and simulation (*5*–*8*), and quantum metrology and sensing (*9*, *10*). With the development of quantum technologies, the requirement for both entanglement dimensionality and photon number increases, demanding large-scale, controllable, and stable quantum photonic sources (*11*, *12*). For example, quantum communication and imaging require photons with high-dimensional entanglement, which can be achieved by using different degrees of freedom of photons, including orbital angular momentum (OAM), time-bin, energy-time, frequency mode, and optical paths. However, none of these meets the requirement of high fidelity with large dimensionality for practical applications. Photonic quantum computation and metrology rely on multiphoton states, which can be synthesized with multiple single-photon sources from spontaneous parametric processes in nonlinear materials or by time-multiplexing the spontaneous emission of quantum dots (*13*), but the largest photon number is limited to ~20 (*14*). Although quantum dots show excellent performance in generating single photons, the spontaneous parametric process continues to be the main method for the generation of high-dimensional and/or multiphoton entangled states (*13*). Recent progress on integrated photonic systems based on such a process provides an ideal platform for large-scale quantum-optical sources (*15*).

Metasurfaces consist of a dense arrangement of dielectric or metallic subwavelength antennas in an ultrathin interface (*16*). By controlling the phase distribution, metasurfaces have been widely used to manipulate the wavefront of a light field (*17*–*23*). Metasurfaces have also found applications in the nonclassical region (*24*–*27*). However, quantum photonic sources based on metasurfaces have not yet been demonstrated.

Here, by using a metalens array, we demonstrate a 100-path spontaneous parametric down-conversion (SPDC) photon source. The 100-path SPDC photon source is realized by combining a metalens array with a 0.5-mm type II β-barium borate (BBO) crystal (Fig. 1, A to D). The metalens array consists of 100 designed metalenses (arranged in a 10 × 10 array), composed of GaN nanopillars fabricated by electron beam lithography (EBL), dry etching, and resist removing (*13*). Each metalens is designed with a uniform focal length of f = 1.1 mm at a working wavelength of 404 nm and an area of 100 μm by 100 μm. The period of the unit element is 200 nm and the height of the nanopillars is 800 nm [design details of the metalens are in the supplementary materials (*13*)]. The image of the focal spot array of the pump laser, with a wavelength of 404 nm (Fig. 1E), shows that the measured focusing efficiency of each metalens has a uniform value of 56.0 ± 6.6%, owing to the precise fabrication (fig. S1).

When a pump laser is incident on the metalens array, a 10 × 10 array of focal spots is formed inside the BBO crystal. Each of the spots can trigger a SPDC process and generate a pair of photons in a probabilistic manner. The phase-matching condition of the BBO crystal is designed to ensure that each photon pair has two well-defined beam-like spatial modes (*28*). The uniform intensity and spatial distributions of these focal spots enable the further realization of high-dimensional entangled and multiphoton quantum photonic sources. As a preliminary test, a vertically polarized diode laser (404 nm, 100 mW) is incident on the metalens–BBO system. An array of 10 × 10 SPDC photon pairs with nearly equal intensities is observed with an electron-multiplying charge-coupled device (EMCCD) (Fig. 1F).

First, the path-encoded quantum entanglement is demonstrated. Each metalens in the system generates a pair of photons in a pair of conjugate spatial modes (figs. S2 and S3). These modes are defined as s_0 to s_{99} for the signal photon (vertically polarized) and as i_0 to i_{99} for the idler photon (horizontally polarized). In the case that only one pair of photons is generated from the source, without knowing which metalens the photons are generated from, the two-photon state can be written as $\frac{1}{10}(|0,0\rangle + |1,1\rangle + |2,2\rangle + \ldots + |99,99\rangle)$, where the number represents the path defined previously. This state is a 100-dimensional path-encoded quantum entangled state. As a demonstration, we verify the quantum entanglement in two, three, and four dimensions by reconstructing the reduced quantum states with quantum state tomography (QST) measurements and discuss the high-dimensional entanglement measurement in the supplementary materials (*13*).

Two-dimensional (2D) entanglement states are analyzed using photon pairs generated by two metalenses, including the adjacent and nonadjacent ones. The QST measurements are performed (fig. S4) and the corresponding density matrix is accurately reconstructed by the maximum likelihood estimation (MLE) method. Figure 2A shows the experimental result of a maximally 2D path-entangled state of $(|00\rangle + |11\rangle)/\sqrt{2}$. The fidelity between the reconstructed state and the ideal maximally entangled state is as high as 0.985, proving that the produced state is very close to the ideal state. In addition to focusing the pump light,

[1]National Laboratory of Solid State Microstructures, School of Physics, College of Engineering and Applied Sciences, Nanjing University, Nanjing, 210093, China. [2]Department of Electronic and Information Engineering, The Hong Kong Polytechnic University, Hong Kong. [3]Research Center for Applied Sciences, Academia Sinica, Taipei 11529, Taiwan. [4]State Key Laboratory of Precision Spectroscopy, School of Physics and Electronic Science, East China Normal University, Shanghai, 200062, China. [5]Key Laboratory of Intelligent Optical Sensing and Manipulation, Ministry of Education, Nanjing University, Nanjing, 210093, China. [6]Collaborative Innovation Center of Advanced Microstructures, Nanjing, 210093, China. [7]Key Laboratory of Quantum Information, CAS, University of Science and Technology of China, Hefei, 230026, China. [8]Synergetic Innovation Center of Quantum Information & Quantum Physics, University of Science and Technology of China, Hefei, 230026, China. [9]Department of Electrical Engineering, National United University, Miaoli 36003, Taiwan. [10]Department of Physics, National Taiwan University, Taipei 10617, Taiwan.
*These authors contributed equally to this work.
†Corresponding author. Email: wangshuming@nju.edu.cn (S.W.); lijian.zhang@nju.edu.cn (L.Z.); zlwang@nju.edu.cn (Z.W.); zhusn@nju.edu.cn (S.Z.); dinping.tsai@polyu.edu.hk (D.P.T.)

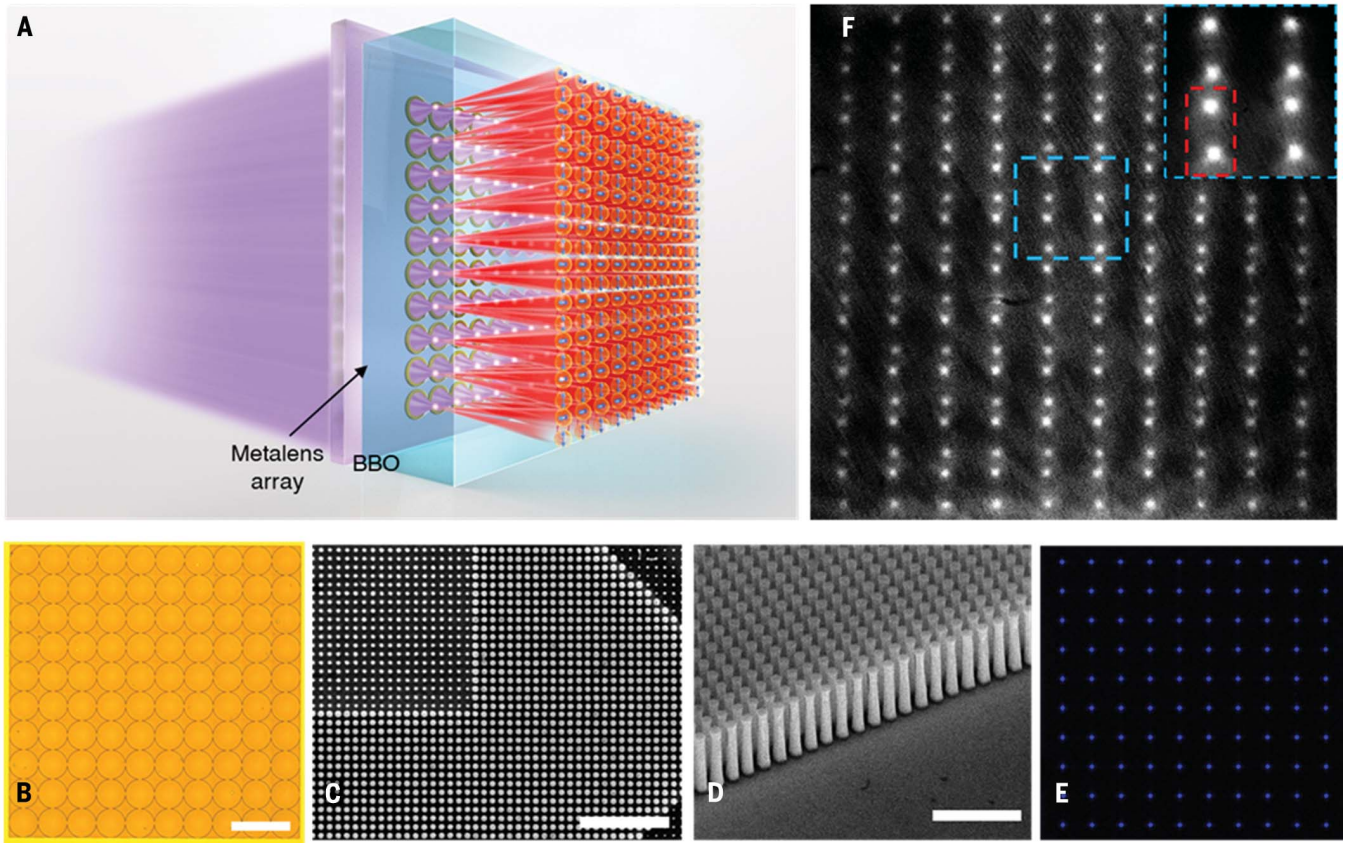

Fig. 1. Schematic and characterization of the quantum metalens array. (**A**) Schematic of the quantum source based on a metalens array. (**B**) Microscopy image of the metalens array. (**C** and **D**) Scanning electron microscopy image of the GaN metalens in (C) top view and (D) side view. (**E**) Microscopy image of the focal plane of the pump light. (**F**) Image of the SPDC photon pair array recorded by EMCCD. Inset: Magnified image of the area indicated by the blue dashed box. The red dashed box shows one pair of photons generated by one metalens. Scale bars: (B) 200 μm, (C) 2 μm, (D) 1 μm.

the metalens is able to encode its phase, which in turn controls the relative phase between different terms of the generated quantum state. We design the metalenses with different phase differences ($\Delta\varphi = \pi/2, \pi, 3\pi/2$) between two adjacent metalenses and analyze the 2D entanglement states generated with them (figs. S5 and S6). Figure 2, B to D, are the reconstructed density matrixes of the prepared states, with the phase differences of ($\Delta\varphi = \pi/2, \pi, 3\pi/2$), respectively. All these density matrixes show good agreement with the ideal corresponding states of $(|00\rangle + i|11\rangle)/\sqrt{2}$, $(|00\rangle - |11\rangle)/\sqrt{2}$ and $(|00\rangle - i|11\rangle)/\sqrt{2}$, respectively. Without loss of generality, we measure six 2D entangled states, with respect to adjacent metalenses pairs at random locations, for each phase difference and estimate them by the QST measurements. All the results show high fidelities, with an average value of 0.979, to the maximally entangled states and a fidelity of 0.984 to the closest pure entangled states (fig. S6). Other results with nonadjacent metalens pairs are shown in fig. S7. The fidelities to the maximally entangled states are all above 0.96 (*13*). These high fidelities confirm that we can reliably control the generated states by metananostructure.

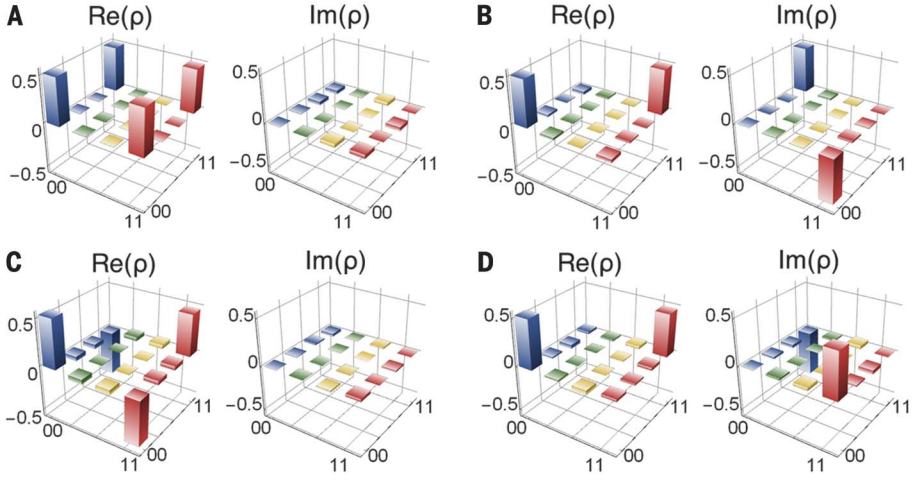

Fig. 2. Characterization of entangled quantum states. (**A** to **D**) Typical reconstructed density matrixes by QST measurements with metalens phase differences of $\Delta\varphi$ = 0, $\pi/2$, π, and $3\pi/2$, respectively. The quantum state fidelities are 0.985, 0.987, 0.987, and 0.984 to the maximally entangled states, respectively.

Quantum entangled states with higher dimensions are further characterized. Figure 3, B and D, are typical 3D and 4D density matrixes reconstructed by QST measurements and correspond to the configuration of the photon pair sources in the dashed boxes in Fig. 3, A and C, respectively. In these high-dimensional cases, the beam displacer (BD)–based measurement setup becomes considerably more complex, as shown in the inset of fig. S4. There are not

enough degrees of freedom to balance the additional accumulation of experimental fluctuations introduced by the BD-based spatial mode combing and analyzing systems. It is a challenge to reconstruct ideal density matrixes of the maximally entangled states. Here, the reconstructed results show very high fidelities to the pure quantum states. The fidelities to the estimated pure states are 0.966 for the 3D entangled state (Fig. 3B) and 0.950 for the 4D entangled state (Fig. 3D), and the fidelities to the maximally entangled states are 0.965 and 0.911, respectively. These results, in addition to the measured results in the supplementary materials (*13*), show entangled fidelities higher than 0.94 to the closest pure states (figs. S8 and S9), manifesting the high qualities of the high-dimensional entangled states from the metalens-array–based quantum source. The decreases in the measured fidelities are mainly caused by the long QST measurement time for high-dimensional entangled states, in which the drift of the measurement system cannot be ignored. Therefore, characterization of the entanglement in higher dimensions may need to resort to the development of integrated devices (*13*, *29*).

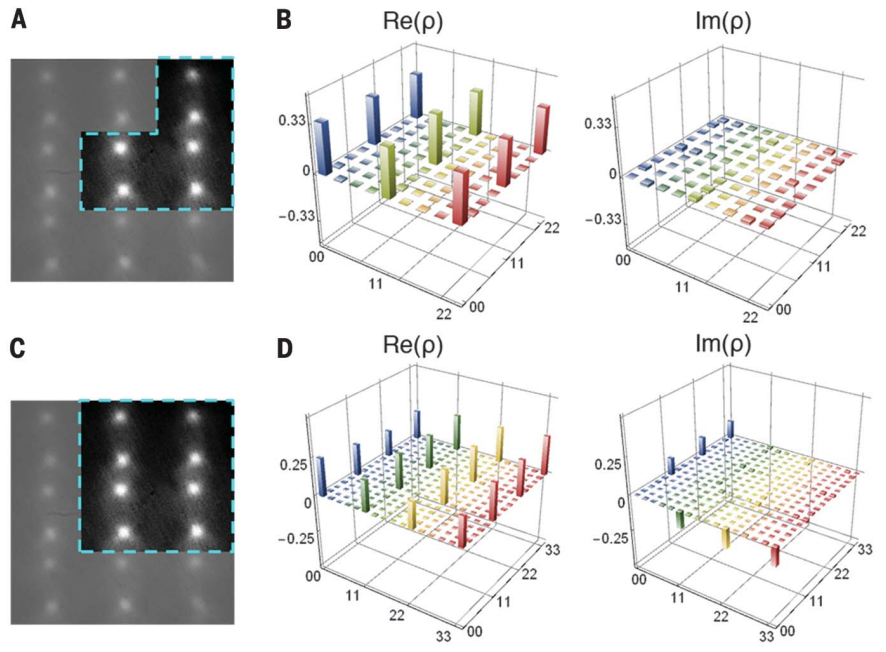

Fig. 3. High-dimensional quantum entanglement states characterization. (**A** to **D**) Reconstructed density matrixes for 3D (B) and 4D (D) quantum state by QST measurements corresponding to the photon pairs in the dashed blue boxes in (A) and (C), respectively.

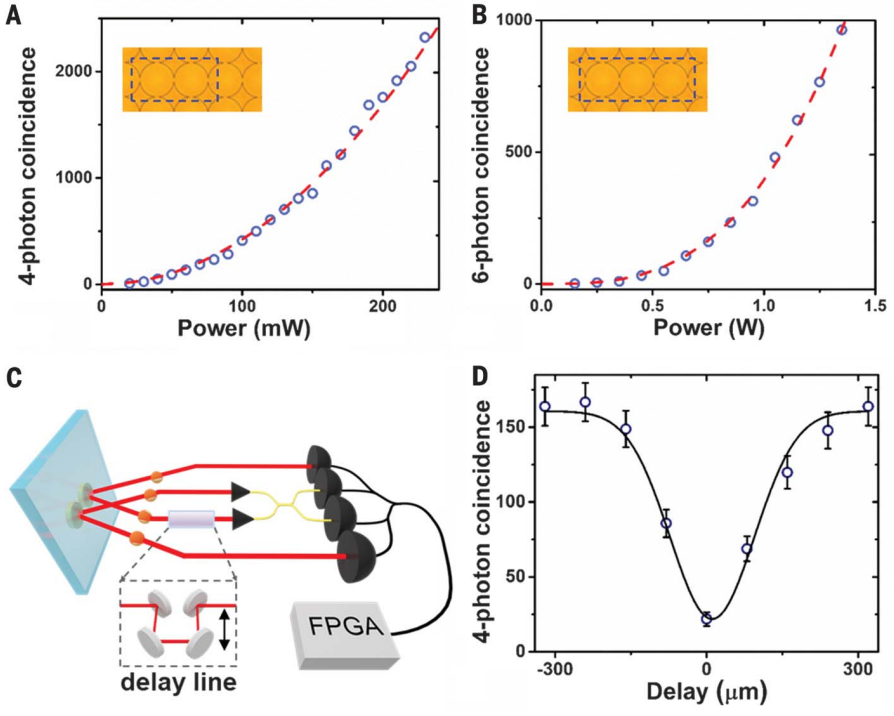

Fig. 4. Multiphoton quantum source based on a metalens array. (**A**) Four-photon and (**B**) six-photon coincidence dependence to the pump power. The red dashed lines are the theoretical estimation of quadratic (four-photon) and cubic (six-photon) trend. The insets show the metalenses involved in the corresponding tests. The schematic diagram (**C**) and the fringe (**D**) of the HOM interference measurement.

Furthermore, the multiphoton source based on the metalens array system is characterized. Unlike the general SPDC-based multiphoton sources, in which multiple nonlinear crystals and long-time stable complex optical setup are required (*14*), our source only needs one nonlinear crystal and the setup is substantially more compact and stable. The experimental setup is discussed in the supplementary materials (*13*), where a 415-nm femtosecond pulsed laser is introduced as the pump light to increase the possibility for multiphoton generation (fig. S10). Here, we use the same metalens array sample shown in Fig. 1 and the BBO crystal designed for the 415-nm pump laser (*13*). Because each metalens may generate one photon pair simultaneously, we can obtain multiphoton-pair sources within this 100-metalens array. As a demonstration, we characterize the performance of the four-photon and six-photon source from two and three adjacent metalenses, respectively. Figure 4, A and B, show the pump power dependencies of the four-photon and six-photon coincidence counts. The ideal power dependencies of the four-photon and six-photon coincidence counts follow a quadratic and cubic relationship, respectively, as shown in the red dashed lines in Fig. 4, A and B. The measured data, shown in the blue circles, agree well with the ideal trend, indicating a feasible multiphoton source.

We further carry out the Hong-Ou-Mandel (HOM) interference to test the purity and indistinguishability of photons generated from different metalenses. Two independent photon pairs are generated by two adjacent metalenses (Fig. 4C). One photon from each pair is used as the trigger (heralding), and two heralded photons interfere at a 50:50 fiber beam splitter. The HOM interference is observed by recording the fourfold coincidence as a function of the relative delay between the heralded photons. Figure 4D is the measured HOM interference result, and the visibility of the HOM dip is 86.3%. This clearly verifies the performance of the multiphoton quantum source and indicates

that such metalens array can successfully provide a compact platform for the multiphoton source preparation.

On the basis of the metalens array, we demonstrate a compact, stable, and controllable platform for a quantum optical source in both high-dimensional entanglement and multiphotons, which extends the spatial configuration and entanglement dimensionality of the integrated path-encoded quantum source. Our results indicate that metasurface structures can provide a route for the generation and control of complex quantum states, not only increasing the quantum system dimensionality but also allowing for the coherent control of multiple photons, thus providing a compact and practical platform for the development of advanced on-chip quantum photonic information processing.

REFERENCES AND NOTES

1. N. Gisin, G. Ribordy, W. Tittel, H. Zbinden, *Rev. Mod. Phys.* **74**, 145–195 (2002).
2. N. Gisin, R. Thew, *Nat. Photonics* **1**, 165–171 (2007).
3. V. Scarani *et al*., *Rev. Mod. Phys.* **81**, 1301–1350 (2009).
4. H. Lo, M. Curty, K. Tamaki, *Nat. Photonics* **8**, 595–604 (2014).
5. E. Knill, R. Laflamme, G. J. Milburn, *Nature* **409**, 46–52 (2001).
6. J. L. O'Brien, *Science* **318**, 1567–1570 (2007).
7. A. Aspuru-Guzik, P. Walther, *Nat. Phys.* **8**, 285–291 (2012).
8. I. M. Georgescu, S. Ashhab, F. Nori, *Rev. Mod. Phys.* **86**, 153–185 (2014).
9. V. Giovannetti, S. Lloyd, L. Maccone, *Nat. Photonics* **5**, 222–229 (2011).
10. S. Pirandola, B. R. Bardhan, T. Gehring, C. Weedbrook, S. Lloyd, *Nat. Photonics* **12**, 724–733 (2018).
11. S. Khasminskaya *et al*., *Nat. Photonics* **10**, 727–732 (2016).
12. M. Malik *et al*., *Nat. Photonics* **10**, 248–252 (2016).
13. Materials, methods, and additional information are available as Supplementary Materials.
14. H. Wang *et al*., *Phys. Rev. Lett.* **123**, 250503 (2019).
15. J. Wang *et al*., *Science* **360**, 285–291 (2018).
16. N. Yu *et al*., *Science* **334**, 333–337 (2011).
17. N. Yu, F. Capasso, *Nat. Mater.* **13**, 139–150 (2014).
18. A. Arbabi, Y. Horie, M. Bagheri, A. Faraon, *Nat. Nanotechnol.* **10**, 937–943 (2015).
19. G. Zheng *et al*., *Nat. Nanotechnol.* **10**, 308–312 (2015).
20. S. Wang *et al*., *Nat. Commun.* **8**, 187 (2017).
21. S. Wang *et al*., *Nat. Nanotechnol.* **13**, 227–232 (2018).
22. R. J. Lin *et al*., *Nat. Nanotechnol.* **14**, 227–231 (2019).
23. M. Khorasaninejad *et al*., *Science* **352**, 1190–1194 (2016).
24. P. K. Jha, X. Ni, C. Wu, Y. Wang, X. Zhang, *Phys. Rev. Lett.* **115**, 025501 (2015).
25. K. Wang *et al*., *Science* **361**, 1104–1108 (2018).
26. T. Stav *et al*., *Science* **361**, 1101–1104 (2018).
27. P. Georgi *et al*., *Light Sci. Appl.* **8**, 70 (2019).
28. X. L. Niu, Y. F. Huang, G.-Y. Xiang, G.-C. Guo, Z. Y. Ou, *Opt. Lett.* **33**, 968–970 (2008).
29. H. Tang *et al*., *Sci. Adv.* **4**, eaat3174 (2018).

ACKNOWLEDGMENTS

Funding: The authors acknowledge financial support from the National Program on Key Basic Research Project of China (2017YFA0303700, 2016YFA0301700, 2018YFA030602, 2019YFA0308704), National Natural Science Foundation of China (no. 11621091, 11822406, 11834007, 11774164, 61590932, 11774333, 11690032, 91836303, 61490711), Anhui Initiative in Quantum Information Technologies (No. AHY130300), the Strategic Priority Research Program of the Chinese Academy of Sciences (no. XDB24030601), and Shenzhen Science and Technology Innovation Commission (no. SGDX2019081623281169).
Author contributions: L.L., Z.L., X.R., and S.W. contributed equally to this work. L.L., S.W., M.-K.C., C.H.C., H.Y.K., and D.P.T. conceived and performed the design, numerical calculation, and classical optical characterization of metalens array. V.-C.S., C.H.C., and M.K.C. fabricated the metalens array samples. L.L., Z.L., X.R., L.Z., S.W., B.L., and W.Z. performed the quantum measurement and the data analysis. S.W., L.Z., Z.W., G.G., S.Z., and D.P.T. organized and led the project. L.L., S.W., Z.L., X.R., L.Z., S.Z., and D.P.T. prepared the manuscripts; all authors discussed the results and commented on the manuscript. **Competing interests:** The authors declare no competing financial interests. **Data and materials availability:** All data are available in the manuscript or the supplementary materials.

SUPPLEMENTARY MATERIALS

science.sciencemag.org/content/368/6498/1487/suppl/DC1
Materials and Methods
Figs. S1 to S10
Table S1

20 January 2020; accepted 1 May 2020
10.1126/science.aba9779

Science

Metalens-array–based high-dimensional and multiphoton quantum source

Lin Li, Zexuan Liu, Xifeng Ren, Shuming Wang, Vin-Cent Su, Mu-Ku Chen, Cheng Hung Chu, Hsin Yu Kuo, Biheng Liu, Wenbo Zang, Guangcan Guo, Lijian Zhang, Zhenlin Wang, Shining Zhu and Din Ping Tsai

Science **368** (6498), 1487-1490.
DOI: 10.1126/science.aba9779

Metalens-array–based quantum source

Spontaneous down-conversion is an exotic optical process in a nonlinear crystal in which a high-energy photon splits into two lower-energy photons that are quantum mechanically entangled. These entangled pairs are valuable commodities for quantum information processing and quantum communications. Because the experimental setup is usually performed with bulk optical components, there is a need to decrease the size scale for application. Li *et al.* combined an array of specialized metalenses with a nonlinear crystal and show that the scale of the process can be shrunk substantially. The approach should prove useful for developing miniaturized integrated quantum optical technologies.

Science, this issue p. 1487

Science (print ISSN 0036-8075; online ISSN 1095-9203) is published by the American Association for the Advancement of Science, 1200 New York Avenue NW, Washington, DC 20005. The title *Science* is a registered trademark of AAAS.